The Journal of Experimental Biology 206, 2595-2609

doi:10.1242/jeb.00474

Reduction in muscle fibre number during the adaptive radiation of notothenioid fishes: a phylogenetic perspective

Ian A. Johnston[1,*], Daniel A. Fernández[1,†], Jorge Calvo[2], Vera L. A. Vieira[1], Anthony W. North[3], Marguerite Abercromby[1] and Theodore Garland, Jr[4]

[1]*Gatty Marine Laboratory, Division of Environmental and Evolutionary Biology, School of Biology, University of St Andrews, St Andrews, Fife, KY16 8LB, Scotland, UK,* [2]*Centro Austral de Investigaciones Cientificas (CADIC), Consejo Nacional de Investigaciones Cientificas y Tecnicas (CONICET) CC92, Ushuaia, 9410, Tierra del Fuego, Argentina,* [3]*British Antarctic Survey, High Cross, Madingley Road, Cambridge, CB3 OET, UK* and [4]*Department of Biology, University of California, Riverside, CA 92521, USA*

*Author for correspondence (e-mail: iaj@st-and.ac.uk)

†Present address: Biology Department, Wesleyan University, Hall-Atwater and Shanklin Laboratories, Middletown, 06459, CT, USA

Accepted 30 April 2003

Summary

The fish fauna of the continental shelf of the Southern Ocean is dominated by a single sub-order of Perciformes, the Notothenioidei, which have unusually large diameter skeletal muscle fibres. We tested the hypothesis that in fast myotomal muscle a high maximum fibre diameter (FD_{max}) was related to a reduction in the number of muscle fibres present at the end of the recruitment phase of growth. We also hypothesized that the maximum fibre number (FN_{max}) would be negatively related to body size, and that both body size and size-corrected FN_{max} would show phylogenetic signal (tendency for related species to resemble each other). Finally, we estimated ancestral values for body size and FN_{max}. A molecular phylogeny was constructed using 12S mitochondrial rRNA sequences. A total of 16 species were studied from the Beagle Channel, Tierra del Fuego (5–11°C), Shag Rocks, South Georgia (0.5–4°C), and Adelaide Island, Antarctic Peninsula (–1.5 to 0.5°C). The absence of muscle fibres of less than 10 μm diameter was used as the criterion for the cessation of fibre recruitment. FD_{max} increased linearly with standard length (SL), reaching 500–650 μm in most species. Maximum body size was a highly significant predictor of species variation in FN_{max}, and both body size and size-corrected FN_{max} showed highly significant phylogenetic signal (P<0.001). Estimates of trait values at nodes of the maximum likelihood phylogenetic tree were consistent with a progressive reduction in fibre number during part of the notothenioid radiation, perhaps serving to reduce basal energy requirements to compensate for the additional energetic costs of antifreeze production. For example, FN_{max} in *Chaenocephalus aceratus* (12 700±300, mean ± S.E.M., N=18) was only 7.7% of the value found in *Eleginops maclovinus* (164 000±4100, N=17), which reaches a similar maximum length (85 cm). Postembryonic muscle fibre recruitment in teleost fish normally involves stratified followed by mosaic hyperplasia. No evidence for this final phase of growth was found in two of the most derived families (Channichthyidae and Harpagiferidae). The divergence of the notothenioids in Antarctica after the formation of the Antarctic Polar Front and more recent dispersal north would explain the high maximum diameter and low fibre number in the derived sub-Antarctic notothenioids. These characteristics of notothenioids may well restrict their upper thermal tolerance, particularly for *Champsocephalus esox* and similar Channichthyids that lack respiratory pigments.

Key words: Antarctic teleosts, growth, muscle fibre recruitment, Notothenioid fishes, phylogeny, skeletal muscle.

Introduction

In teleost fish, postembryonic growth of the myotomal muscle involves the recruitment and expansion of muscle fibres, a process that continues during juvenile and adult stages (Rowlerson and Veggetti, 2001; Johnston, 2001). Initially, muscle fibres are produced from discrete germinal zones by stratified hyperplasia (Rowlerson and Veggetti, 2001). The major mechanism for expanding fibre number in most species is mosaic hyperplasia, which involves the activation and proliferation of myogenic precursor cells that are widely scattered throughout the myotome (Rowlerson et al., 1995; Johnston et al., 1999). Myogenic cells withdraw from the cell cycle and fuse to form myotubes on the surface of existing muscle fibres (Koumans and Akster, 1995). In each of 10 species of freshwater fish that have been studied, mosaic hyperplasia was shown to cease at around 44% of the maximum body length, and the final stages of growth were

entirely supported by fibre hypertrophy (Weatherley et al., 1988). The maximum diameter of each muscle fibre type is related to ultimate body size and is probably limited by diffusional constraints reflecting metabolic demand and temperature (Archer and Johnston, 1991).

The fish fauna of the continental shelf of the Southern Ocean is dominated by a single sub-order of Perciformes, the Notothenioidei, which comprises at least 125 species divided into eight families (Eastman and Eakin, 2000). Several authors have reported that Antarctic notothenioids have unusually large diameter fibres, which can reach 100 μm in slow muscle and 500 μm in fast muscle (Smialovska and Kilarski, 1981; Dunn et al., 1989; Battram and Johnston, 1991). Slow muscle fibres have relatively high densities of mitochondria (Johnston, 1987; Archer and Johnston, 1991; O'Brien et al., 2003), reaching 50% of fibre volume in some Channichthyids (haemoglobin-less icefishes) (Johnston, 1989). However, mitochondria are found in the central zone of even the largest-diameter slow fibres (Johnston, 1987; Archer and Johnston, 1991), consistent with the maintenance of adequate tissue oxygenation at the low body temperature of these species (Egginton et al., 2002). Fast muscle fibres with diameters of 400 μm have also been reported in sub-Antarctic notothenioids from the Beagle Channel, although a relatively restricted size range of fish was studied (Fernández et al., 2000).

The ancestral form of the notothenioids is generally considered to have been a temperate bottom-living species without a swim bladder (Eastman, 1993). The success of the radiation of the Antarctic notothenioids has been attributed to the evolution of glycopeptide and peptide antifreezes, which enabled them to adjust to the climatic cooling that occurred following the opening of the Drake passage and establishment of the Antarctic Polar Front (APF) some 20–25 million years ago (Cheng and DeVries, 1991; Eastman, 1993; Clarke and Johnston, 1996). The Bovichtidae, Pseudaphritidae and Eleginopidae are the most basal notothenioid families and, except for a single Antarctic species of bovichtid, are represented by non-Antarctic species with the plesiomorphic condition of lacking antifreezes (Eastman and Eakin, 2000).

Members of six families of notothenioids are found outside the Antarctic in the Beagle Channel, Patagonian Shelf, along the Pacific Coast of South America and in the sub-Antarctic waters of New Zealand (Eastman, 1993). One bathypelagic species, the Patagonian toothfish *Dissostichus eleginoides* (Nototheniidae), grows to 2 m total length and occurs on both sides of the Polar Front, from a latitude of 40°S off the coasts of S. America to 60°S south in the Antarctic. The distribution of *D. eleginoides* is circum-Antarctic and its range overlaps with a sister species *D. mawsoni* that is found around the Antarctic continental shelf (Fisher and Hureau, 1985). Evidence from a molecular phylogeny estimated using mitochondrial 12S and 16S rRNA DNA sequences suggests that many sub-Antarctic species evolved subsequent to the main radiation of the group, as recently as 7–9 million years ago (Bargelloni et al., 2000; Stankovic et al., 2001).

It has been suggested that the radiation of the Antarctic notothenioids has been associated with a loss of characters or evolutionary function (disaptation) followed by subsequent adaptive recovery (Montgomery and Clements, 2000). Within the notothenioids, the family Channichthyidae (icefishes) is notable for the loss of haemoglobin, which is thought to have resulted from a single mutational event that deleted the entire β-globin gene and the 5′ end of the linked α-globin gene (Cocca et al., 1995). Loss of respiratory pigments is associated with a suite of compensatory adaptations in the heart and peripheral circulatory system (Tota et al., 1997). These include a relatively large ventricular muscle mass (Johnston et al., 1993), a high blood volume (Acierno et al., 1995), coupled to a high output cardiac pump operating at low frequencies and pressures (Tota et al., 1997). Six of the 15 species of icefishes also lack myoglobin in their heart muscle (Moylan and Sidell, 2000), involving at least three independent mechanisms including a 5-nucleotide insertion leading to premature termination in *Champsocephalus gunnari*, an aberrant polyadenylation signal in *Pagetopsis macropterus* (Vayda et al., 1997), and a duplicated TATAAAA sequence that interferes with transcription in *Chaenocephalus aceratus* (Small et al., 2003). Some notothenioids have undergone an ecological diversification to feed in the water column involving changes in body shape, colour, and the attainment of near neutral buoyancy through decreased mineralisation of the skeleton and the accumulation of lipids (Eastman, 1993, 1997; Klingenberg and Ekau, 1996). In some cases secondary pelagicism is associated with the retention of larval characteristics into adult stages (Eastman, 1993; Montgomery and Clements, 2000), The resulting detrimental changes to the lateral line sensory system have been compensated for by changes in central processing mechanisms and behaviour (Montgomery and Clements, 2000).

The first aim of the present study was to test the hypothesis that a high maximum fibre diameter in notothenioid fishes was related to a reduction in the number of muscle fibres at the end of the recruitment phase of growth (FN_{max}). We then used phylogenetically based statistical methods to test whether fibre number was negatively related to body size and whether either body size or size-corrected fibre number showed significant phylogenetic signal. Finally, we estimated ancestral values for body size and fibre number to explore where during the evolutionary radiation reductions in fibre number occurred. A total of 16 species of Notothenioidei from three geographical provinces were studied, including representatives with benthic and secondarily pelagic lifestyles, and an independent phylogeny was constructed using sequence information from mitochondrial 12S rRNA genes.

Materials and methods

Fish

Fish of the suborder Notothenioidei (order Perciformes) were caught in three geographical regions; near Ushuaia,

Beagle Channel, and Atlantic coast Tierra del Fuego, Argentina (54°49′S, 68°13′W), Shag Rocks, South Georgia (54°33′S, 42°02′W) and Rothera Research Station, Adelaide Island, Antarctic Peninsula (67°34′S, 68°08′W) (Fig. 1). All fish were captured during the austral summer (December–February). Fish from the Beagle Channel were obtained in 1999, 2000 and 2001 using a mixture of baited traps and trammel nets. The following species were studied: *Eleginops maclovinus* Cuvier in Cuvier and Valenciennes 1830, *Patagonotothen tessellata* Richardson 1845, *Patagonotothen longipes* species complex Steindachner 1876, *Patagonotothen sima* Richardson 1844; *Cottoperca gobio* Günther 1861, *Champsocephalus esox* Günther 1861, *Harpagifer bispinis* Schneider in Bloch and Schneider 1801 and *Paranotothenia magellanica* Forster in Bloch and Schneider 1801. Specimens were usually processed immediately or within a few hours of capture. Most of the larger specimens of *E. maclovinus* were caught along the northern Atlantic coast of Tierra del Fuego using trammel nets and were held on ice for up to 24 h prior to processing. Fish were obtained at Shag Rocks, South Georgia from the 2000–2001 ‘Groundfish Survey’ conducted for the Government of South Georgia and the South Sandwich Islands and were caught by bottom trawl at 200 m depth. The species studied were the Patagonian toothfish, *Dissostichus eleginoides* Smitt 1898, *Chaenocephalus aceratus* Lönnberg 1906 and *Champsocephalus gunnari* Lönnberg 1905. They were killed with a blow to the head, sealed in plastic bags, and shipped on ice *via* the Falkland Islands to the UK, where they were processed on the sixth day after capture. The Antarctic species studied were *Notothenia rossii* Richardson 1844, *Notothenia coriiceps* Richardson 1844, *Trematomus newnesi* Boulenger 1902, *Harpagifer antarcticus* Nybelin 1947 and *Pagothenia borchgrevinki* Boulenger 1902. They were caught using a combination of traps, trammel nets and SCUBA divers. Antarctic fish were transported to the UK in cold aquaria aboard the RRS James Clarke Ross and maintained for up to 3 months in St Andrews at –0.5°C (12 h:12 h light:dark). They were fed *ad libitum* on squid and Antarctic krill. Fish were killed by a sharp blow to the head followed by pithing of the central nervous system. The numbers, size range and maximum-recorded length of the fish studied are shown in Table 1. Data on the *Harpagifer* species has been reported in a preliminary publication (Johnston et al., 2002). The satellite images in Fig. 1 for summer and winter show typical mean monthly sea surface temperatures between 1971 and 2001 at the study sites for February and September) (Website: http://iridl.ldeo.columbia.edu/SOURCES/.IGOSS/.nmc/.Reyn_SmithOIv1/.climatology/.sst/) (see Reynolds and Smith, 1994).

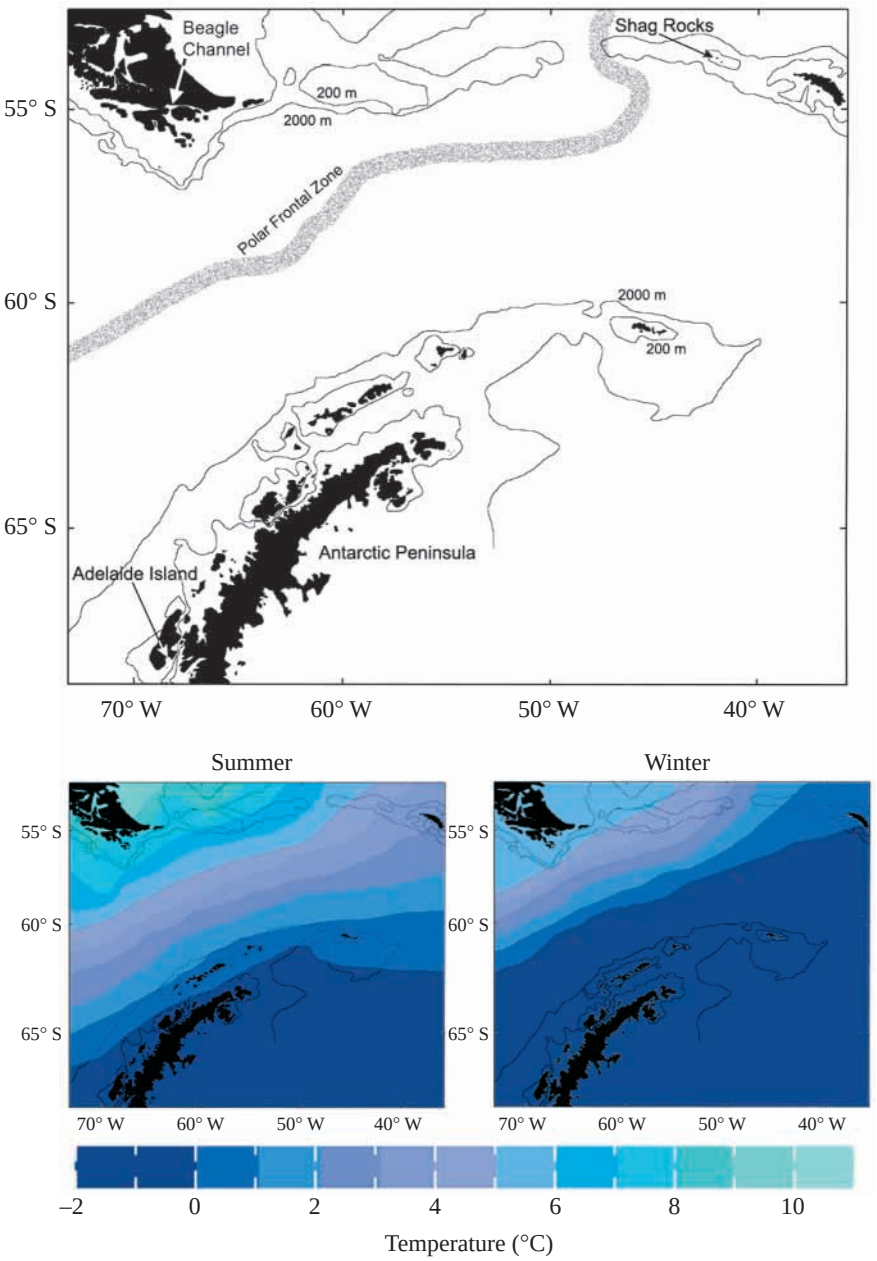

Fig. 1. Sample sites in relation to the Polar Frontal Zone and summer and winter sea surface temperatures represented by the mean of satellite observations between 1971 and 2001 for February and September.

Histology

A 0.5 cm transverse steak of the trunk was prepared at 0.7 standard length (*SL*) using a sharp knife. The steak was either photographed using a digital camera and macro lens or traced

onto an acetate sheet in triplicate. The total area of fast muscle was digitised (TCA). The steak was divided into a series of up to 12 blocks (25 mm^2), depending on the size of the fish, so as to representatively sample all areas of the fast muscle. The number of blocks was adjusted to sample 25–50% of one half of the steak. Blocks were frozen in isopentane (2-methyl butane) cooled to near its freezing point in liquid nitrogen (–159°C). Frozen sections were cut on a cryostat at 7 μm thickness. Preliminary immonohistochemical investigations confirmed the identity of muscle fibre types on the sections. Briefly, sections were stained using standard methods (Johnston et al., 1999) with the S-58 and F-59 antibodies (Crow and Stockdale, 1986), which have been shown to identify slow and fast muscle myosin, respectively, in a wide range of fish species (Devoto et al., 1996; M. Abercromby, unpublished results) (see Fig. 2A,B). For the routine quantification of fibre number, sections were stained with Haematoxylin–Eosin. The cross-sectional areas of 1000 muscle fibres were measured per fish, sampled equally between the blocks and the equivalent fibre diameter computed. The total number of muscle fibres per trunk cross-section was estimated as previously described; reproducibility was approximately 3% (Johnston et al., 1999). Smooth distributions were fitted to the measurements of fibre diameter using a kernel function as previously described (Johnston et al., 1999). Values for the smoothing coefficients showed no systematic variation between species and were within the range 0.085–0.25. The occurrence of muscle fibre recruitment was determined on the basis of the presence of fibres less than 10 μm diameter. The final number of fast muscle fibres (FN_{max}) was the mean ± S.E.M. of the fibre number estimate for all the fish in which fibre recruitment was complete.

Estimation of a molecular phylogeny

Sixteen species of notothenioids belonging to five families were analysed. Partial 12S mitochondrial rRNA sequences of ten notothenioid species were retrieved from GenBank (*E. maclovinus*, AF145426, 341 bp; *D. eleginoides*, AF145425, 340 bp; *P. borchgrevinki*, PBU90411, 390 bp; *T. newnesi*, TNU27527, 374 bp; *P. tessellata*, AF145433, 343 bp; *N. coriiceps*, NCMT12SG, 373 bp; *N. rosii*, AF145432, 341 bp; *C. aceratus*, CAMT12SG1, 373 bp; *C. gunnari*, AF145424, 330 bp; *H. antarcticus*, U37137, 373 bp). cDNAs from six other species were cloned for this study: *C. gobio*, *P. sima*, *P. longipes*, *P. magellanica*, *C. esox* and *H. bispinis*. Two of the sequences (from C. *gobio*, CGU87414, 250 bp, and *C. esox*, CES307046, 309 bp) were already available in GenBank but longer sequences were required to improve the quality of the alignment. The new sequences of 12S mitochondrial rRNA cloned were submitted to GenBank [accession numbers AY22775 (*C. gobio*), AY227776 (*C. esox*), AY227777 (*H. bispinis*), AY227778 (*P. sima*), AY227779 (*P. longipes*) and AY227780 (*P. magellanica*)].

Table 1. *Number, size range and maximum length of the 16 species of notothenioid fish studied*

Species	Number	Size range		Maximum-recorded length (cm)
		Standard length (cm)	Body mass (g)	
Tierra del Fuego				
Cottoperca gobio	2	13.6, 22.8	47.3, 282.9	50[1]
Eleginops maclovinus	57	4.4–64.1	1.05–4183	85[2]
Paranotothenia magellanica	23	9.3–33.9	19.8–928	43[2]
Patagonotothen tessellata	22	3.3–27.6	0.54–446	28[2]
Patagonotothen sima	8	4.5–12.0	1.4–30.9	12[3]
Patagonotothen longipes sp.	9	17.5–27.8	81.3–347	28[3]
Harpagifer bispinis	21	2.5–7.1	0.36–7.2	7[1]
Champsocephalus esox	1	28.2	200.1	35[1]
South Georgia				
Dissostichus eleginoides	25	25.7–62.4	200–3500	200[1]
Chaenocephalus aceratus	17	21.7–72.0	58–4183	84[4]
Champsocephalus gunnari	19	15.6–36.8	28–494	62[4]
Antarctic Peninsula				
Notothenia rossii	1	21.5	234.5	92[4]
Notothenia coriiceps	14	6.2–35.0	4.1–819	58[1]
Pagothenia borchgrevinki	4	18.0–22.5	85.8–112.1	26[1]
Trematomus newnesi	4	11.1–20.8	26.4–193.8	21[1]
Harpagifer antarcticus	13	0.84–10.1	0.008–24.8	12[4]

[1]Gon and Heemstra (1990).
[2]Fernández et al. (2000).
[3]J. Calvo, unpublished results.
[4]British Antarctic Survey Archives.

Reverse transcriptase–polymerase chain reaction

Total muscle RNA was isolated using Qiagen Rneasy Mini and Midi Kits. First-strand cDNA synthesis was carried out using 3′ rapid amplification of cDNA ends system (RACE, Gibco BRL, Life Technologies, Gaitheisburg, USA). Polymerase chain reaction (PCR) was performed using two sets of primers. The first set was Forward 5′-AAAAAGCTTCAAACTGGGATTAGATACCCCACTAT-3′ and Reverse 5′-TGAGTCAGAGGGTGACGGGGCGGTGT-3′ (Ritchie et al., 1997). The second set was Forward 5′-GCGTAAAGGGTGGTTAGG-3′ and Reverse 5′-TCTTA-CTGCTAAATCCTCC-3′ (Stankovik et al., 2001). The PCR cycles used for the first primer set were 94°C for 2 min for denaturation, 35 cycles of 94°C for 30 s, 61°C for 30 s and 72°C for 1 min and elongation at 72°C for 5 min. The PCR cycles used for the second primer set were 94°C for 2 min for denaturation, 35 cycles of 94°C for 30 s, 49°C for 30 s and 72°C for 1 min and elongation at 72°C for 5 min. In all PCRs a proof-reading TAQ polymerase was used (Pfu from Promega UK, Southampton, UK). DNA sequencing was performed in triplicate by The Sequencing Service (School of Life Sciences, University of Dundee, Scotland; http://DNASEQ.biocehm.dundee.ac.uk) using DYEnamic ET terminator chemistry (Amersham Biosciences, Chalfont St Giles, Bucks, UK) on Applied Biosystems automated DNA sequencers.

Alignment

The DNA sequences were put together in a FASTA file using BioEdit (Hall, 1999) and aligned using ClustalW at EMBL (http://www.ebi.ac.uk/clustalw/) with default parameters. The alignment was checked by eye using BioEdit in order to be sure the automatic process was correct, and finally reduced to the part of the alignment where most of the specific sequences were represented. The final alignment of the 16 species was 383 bp long. The alignment was used as the input for the phylogenetic analysis. The database was bootstrapped 100 times using SEQBOOT (Phylip package version 3.6). Maximum likelihood (ML) analysis with a molecular clock assumption to assess divergence times was performed using DNAMLK (Phylip package version 3.6). The analysis was carried out using the following parameters previously calculated in PUZZLE version 5.0: transition/transversion ratio: 2.41, gamma distribution parameter alpha=0.24. The

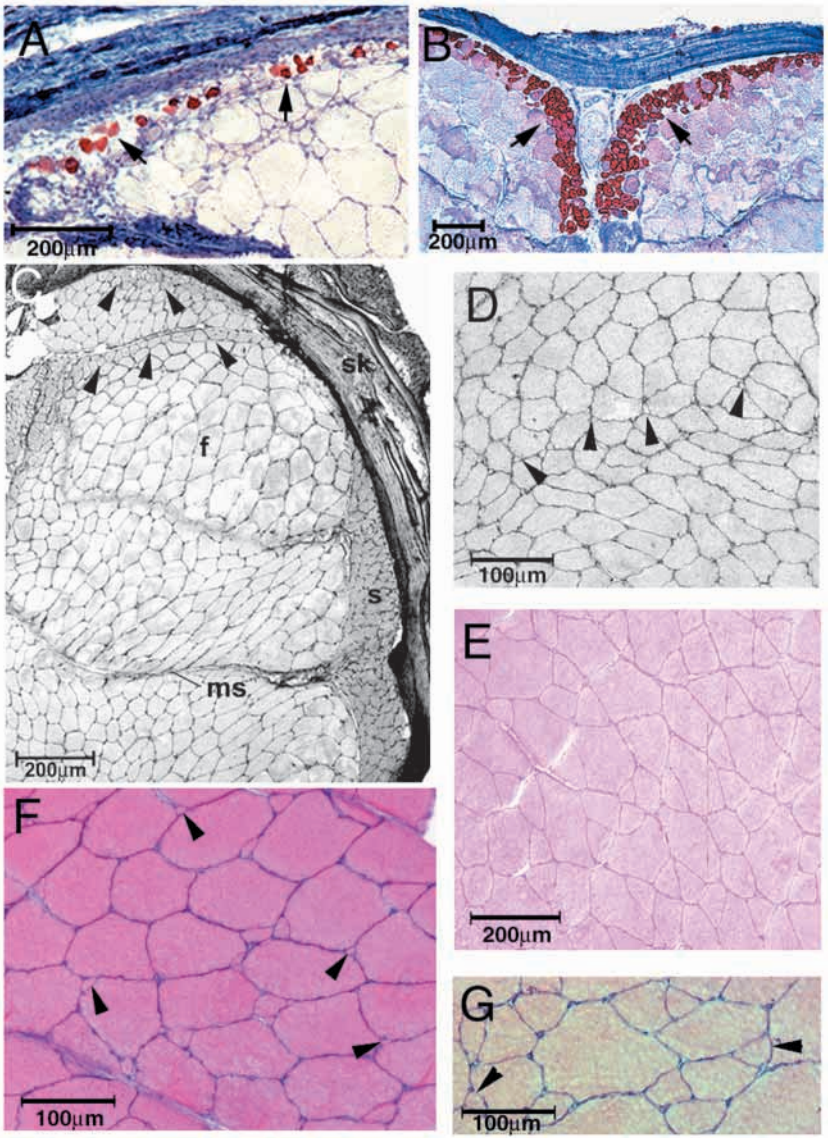

Fig. 2. Phases of growth observed in the myotomal muscle of Antarctic and sub-Antarctic notothenioid fish. (A–G) Transverse sections through the trunk stained with Haematoxylin–Eosin (A) Section from *Notothenia coriiceps*, 11.2 cm standard length (*SL*), stained with the antibody S58, showing the presence of a superficial layer of slow muscle fibres (arrows) dorsal to the major horizontal septum. (B) *Trematomus newnesi*, 13.3 cm *SL*, section stained with S58 showing the slow muscle fibres adjacent to the lateral line nerve (arrows). The fast muscle fibres were counterstained with Haematoxylin–Eosin. (C) Dorsal region of the trunk in a juvenile *Notothenia coriiceps*, 6.0 cm *SL*. The arrowheads indicate zones of stratified hyperplasia containing fibres of smaller diameter than the surrounding tissue. (D) The start of mosaic hyperplasia (arrowheads) in the fast muscle of a juvenile *Notothenia coriiceps*, 6.7 cm *SL*. Note that small diameter satellite fibres are not uniformly distributed through the field of view. (E) The pattern of fibre diameters characteristic of mosaic hyperplasia was still present in *E. maclovinus* of 37.5 cm *SL*. (F) Active mosaic hyperplasia (arrowheads) in the fast muscle of a juvenile *Eleginops maclovinus*, 4.7 cm *SL*. (G) The smallest specimen of *Paranotothenia magellanica* captured, 9.3 cm *SL*, showed a mosaic pattern of fibre diameters (arrowheads). s, slow muscle; f, fast muscle; sk, skin; ms, myosepta. Scale bars, 200 μm (A–C,E); 100 μm (D,F,G).

consensus tree was assembled using CONSENSE (Phylip package version 3.6). The node heights and branch lengths for the final tree used are given in the Appendix.

Statistical analyses

We used both conventional and phylogenetically based statistical analyses. For the latter, the phylogenetic topology estimated as described above (and shown in Fig. 8) was used, and two different sets of branch lengths were considered (see next paragraph). We tested whether $\log_{10}SL_{max}$ and $\log_{10}FN_{max}$ exhibit significant phylogenetic signal (a tendency for related species to resemble each other; Blomberg and Garland, 2002) using the randomization test and associated MatLab program (PHYSIG.M) described in Blomberg et al. (2003) and 1000 permutations. Because $\log_{10}FN_{max}$ was strongly related to $\log_{10}SL_{max}$, we also tested for phylogenetic signal in a size-corrected value of FN_{max}. Following Blomberg et al. (2003), we first determined the allometric scaling exponent for the log–log relationship using phylogenetically independent contrasts (Felsenstein, 1985), calculated with the PDTREE program of Garland et al. (1999). We then divided the value for FN_{max} by SL_{max} raised to the appropriate scaling exponent (b=0.722 for real branch lengths, b=0.964 for constant branch lengths), and then took the log of this value. We used the K statistic of Blomberg et al. (2003) as a descriptor of the amount of phylogenetic signal present in traits. A value of unity indicates that a trait has exactly the amount of signal expected under Brownian motion evolution along the specified topology and branch lengths, whereas values less than unity indicate less signal than expected, and values of K greater than unity indicate more.

As discussed elsewhere, the branch lengths used for phylogenetic analyses need to be tested for statistical adequacy and can have a large effect on the results of analyses (e.g. see Garland et al., 1992, 1999; Diaz-Uriarte and Garland, 1998; Freckleton et al., 2002). The phylogenetic tree estimated as described above includes estimates of branch lengths. These branch lengths may be referred to as ‘real’ because they are derived from data. However, they are derived from data on DNA sequence divergence, whereas phylogenetically based statistical methods require branch lengths in units proportional to expected variance of character evolution for the actual characters (e.g. body size, fibre number) under study (e.g. see Felsenstein, 1985; Garland et al., 1992; Freckleton et al., 2002; Blomberg et al., 2003). Therefore, such ‘real’ branch lengths may or may not perform well for statistical analyses. Hence, as an alternative set of branch lengths, we set all segments to be equal in length (i.e. each segment was set to equal a value of unity). We then compared the statistical performance of these two alternate sets of branch lengths by three criteria. First, we used the diagnostic check suggested by Garland et al. (1992) (see also Diaz-Uriarte and Garland, 1998), which involves plotting the absolute values of standardized phylogenetically independent contrasts (Felsenstein, 1985) *versus* their standard deviations and calculating the correlation coefficient (not through the origin). A correlation closer to zero implies a better fit of the branch lengths to the data. Second, we calculated the mean squared error (MSE) in a generalized least-squares analysis (equivalent to the variance of the standardized contrasts) using PHYSIG.M of Blomberg et al. (2003). Again, a smaller MSE implies a better fit. We considered the foregoing two statistics for $\log_{10}$ maximum length (SL_{max}: data reported in Table 1) because it is the primary independent variable in the analysis and because fibre number was expected to be strongly correlated with SL_{max}. Finally, we examined the independent contrasts regression (through the origin) of $\log_{10}FN_{max}$ on $\log_{10}SL_{max}$. Here, a higher r^2 implies a better fit of the branch lengths to the data (assuming that the data appear to fit the line well, e.g. linearity, homoscedasticity of residuals, lack of outliers or influential points).

We used PDTREE (Garland et al., 1999) to estimate ancestral values and 95% confidence limits for both $\log_{10}SL_{max}$ and $\log_{10}$size-corrected FN_{max}. A clear sister group to the notothenioids has not been identified, although characters may be polarised relative to the Bovichtidae, and this family has often been used as a ‘functional outgroup’ (Eastman, 1993). We therefore compared node 2 in the phylogenetic tree (see Fig. 8), which represents the ancestor of the Eleginopinae, Nototheniidae, Channichthyidae and Harpagiferidae, with node 6, which is the ancestor of the Channichthyidae. Comparison of the 95% confidence limits (c.l.) allowed us to test whether either trait showed a significant change between the two nodes.

Results

Patterns of muscle growth

The stratified hyperplasia stage of growth is characterised by layers of fibres of relatively uniform diameter arising from discrete germinal zones (Fig. 2C). This pattern of growth was found in the smallest specimens of *N. coriiceps*, 6–7 cm standard length (*SL*), in which distinct layers of small diameter (<10 μm) fast fibres were observed adjacent to myosepta at the dorsal (Fig. 2C) and the ventral apices of the trunk (not illustrated). Active stratified hyperplasia was not observed in any of the other species for which juvenile stages were available (*E. maclovinus*, 4.4 cm *SL* and *P. tessellata*, 3.3 cm *SL*). In the remaining species studied, with the exception of the three channichthyids and two *Harpagifer* spp., new small diameter fibres were found on the surface of existing fibres either in restricted zones (illustrated for a juvenile *N. coriiceps* in Fig. 2D) or throughout the myotome (Fig. 2E). The myotomes of juvenile *E. maclovinus* (5–7 cm *SL*) showed fibre addition throughout the myotomal cross-section giving rise to a pattern of fibre diameters typical of mosaic hyperplasia (Fig. 2F). Fibre recruitment in *E. maclovinus* ceased at approximately 26 cm *SL*, equivalent to 31% of the maximum attainable length (SL_{max}) (Table 1). Even in the largest specimen caught (64.1 cm *SL*), the characteristic mosaic pattern of fibre diameters was still discernible (not illustrated).

Another species showing a prolonged period of mosaic

hyperplasia was *D. eleginoides*. Muscle fibres <10 μm diameter were present in specimens 35.6 cm *SL* or less, but absent from fish over 52 cm *SL*. It was not possible to establish the precise length at which fibre recruitment ceased in this species. The complete range of juvenile and adult stages was studied for *P. tessellata* (3.3–27.6 cm *SL*). Fibres less than 10 μm in diameter were only present in the four smallest specimens 3.3–3.5 cm *SL*. This suggests that fibre recruitment ceased between 3.5 and 7.7 cm *SL*, which is equivalent to 12.6–27.9% of the maximum-recorded length. The fast muscle of the smallest specimen of *P. magellanica* studied (9.5 cm *SL*) showed the characteristic mosaic pattern of fibres (Fig. 2G), but there were no fibres less than 10 μm diameter (not shown), indicating fibre recruitment had already ceased at 22% SL_{max}. Only the smallest *N. coriiceps* studied had muscle fibres less than 10 μm diameter, suggesting recruitment had ceased at approximately 16.8% of *SL*.

For all the other species, muscle growth was by fibre hypertrophy alone for the length ranges studied. For Channichthyidae (*Chaenocephalus aceratus*, *Champsocephalus esox* and *C. gunnari*) and the two *Harpagifer* spp., the fibres in particular regions of the myotome were of relatively uniform diameter (illustrated for *C. aceratus* in Fig. 3A). Thus the pattern of fibre diameter characteristic of mosaic hyperplasia was absent, which suggests that postembryonic growth was largely or entirely dependent on stratified hyperplasia.

In the largest individuals of *N. coriiceps* (Fig. 3B), *P. tessellata* (Fig. 3C) and *P. longipes* (not illustrated) the fibres appeared to be undergoing splitting. The connective tissue sheath surrounding each fibre appeared to infiltrate and subdivide the fibre into 2–6 smaller daughter fibres (Fig. 3B,C), and in some cases there were aggregations of nuclei (arrowheads in Fig. 3C). Intermediate stages in this process were also occasionally observed (not shown). The incidence of 'split fibres' in the largest fish remained low (1–3%) and was not sufficient to make a material difference to the estimate of fibre number.

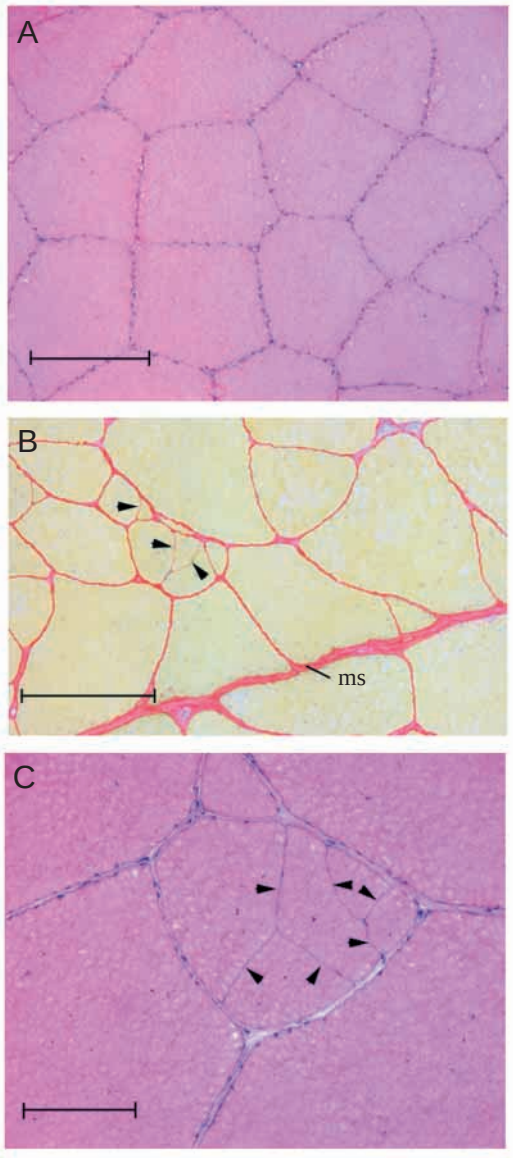

Fig. 3. Phases of growth observed in the myotomal muscle of Antarctic and sub-Antarctic notothenioid fish that have a relatively low final muscle fibre number. (A) Transverse section through the trunk stained with Haematoxylin–Eosin from an adult icefish *Chaenocephalus aceratus*, 27.6 cm standard length (*SL*). Note the relatively uniform distribution of large diameter (approx. 200 μm) muscle fibres. (B) Transverse section of a region of fast muscle fibres from an adult *Notothenia coriiceps*, 35.5 cm *SL*, stained with Scarab Red to visualise collagen fibrils. The arrowheads show the apparent splitting of a fibre into smaller daughter fibres each surrounded by a connective tissue sheath. (C) Transverse section of a region of fast muscle fibres from an adult *Patagonotothen longipes* sp. (27.8 cm *SL*) showing the apparent splitting of a fibre into smaller daughter fibres. Arrowheads indicate the position of myonuclei. ms, myosepta. Scale bars, 200 μm (A,B); 100 μm (C).

Distribution of muscle fibre diameters

Smooth distributions were fitted to measurements of 800–1000 muscle fibres per fish using a kernel function (Fig. 4A,B). The distributions of fast muscle fibre diameters in the juvenile *E. maclovinus* studied were unimodal with a peak density that increased from 10–40 μm diameter over the length range 4.4 (red line in Fig. 4A) to 18.6 cm *SL*. Some evidence for a bimodal distribution of fibre size was observed in fish of 23.4–28 cm *SL* (Fig. 4A). In individuals greater than 26 cm *SL* there were no small diameter fibres, and in the biggest specimens there was a broad unimodal distribution of fibre sizes with a peak ranging from 100 to 200 μm diameter (blue line in Fig. 4A). In contrast, fast fibre diameters in the smallest specimens (3.3–8.6 cm *SL*) of *P. tessellata* were bimodal (red line in Fig. 4B), with the distribution becoming unimodal and broader with increasing SL (green and blue lines in Fig. 4B). Fibres less than 10 μm diameter were not present in fish of 8.6 cm *SL* or larger. In an individual, 27.6 cm *SL*, close to the maximum size reported for this species (Table 1), there was a broad peak to the distribution from 250 to 500 μm diameter (blue line in Fig. 4B). There was also a distinct right-hand peak of fibres 20–100 μm diameter, which was not present in fish

20–23 cm *SL*, probably corresponding to fibres produced by the splitting process illustrated in Fig. 3B,C.

An estimate of the maximum fibre diameter per fish was obtained from the 99th percentile of the distribution and these values were similar to the average value of the 10 largest fibres measured. In all cases the maximum fibre diameter was linearly related to fish standard length (Fig. 5A,B), although there was significant interspecific variation in the slopes and intercepts of the relationships (Table 2). The highest slopes were found in those species with the lowest number of fast fibres per trunk cross-section (Fig. 5A,B) (Table 2). For the species that were close to their maximum body length, FD_{max} was 550 µm in *P. longipes* sp. and 600 µm in *P. tessellata* (Table 2). For the nine species where it could be determined, there was no relationship evident between the geographical zone in which the fish were captured and FD_{max} (Table 2).

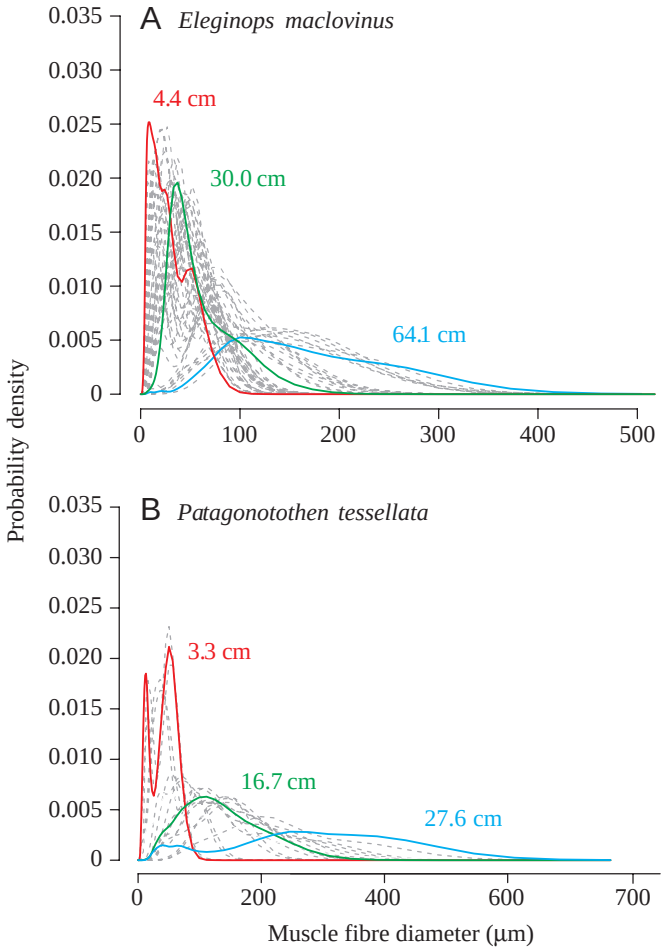

Fig. 4. The distribution of muscle fibre diameters in relation to fish standard length (*SL*, cm) in the fast myotomal muscle of (A) *Eleginops maclovinus* and (B) *Patagonotothen tessellata*. Smooth distributions were fitted to 1000 measurements of muscle fibre diameter using a kernel function. Each dotted line represents an individual fish. The coloured lines represent the smallest (red), the largest (blue) and an intermediate size (green) fish, of indicated *SL*.

Muscle fibre number

FN_{max} was estimated for all 16 species. The change in the number of fast muscle fibres (*FN*) per trunk cross-section in relation to the total cross-sectional area of muscle (TCA) at 0.7 *SL* for three of the species is shown in Fig. 6A–C. Among species, $\log_{10}FN_{max}$ was positively and apparently linearly related to $\log_{10}SL_{max}$ (Fig. 7). Fig. 7 also indicates that size-corrected FN_{max} was apparently unrelated to geographic origin, and inspection of Fig. 8 indicates no obvious relation with locomotory habit.

$\log_{10}SL_{max}$, $\log_{10}FN_{max}$, and $\log_{10}$size-corrected FN_{max} all showed highly significant phylogenetic signal (all $P<0.001$), irrespective of whether the real (as in Fig. 8) or arbitrary branch lengths (each segment length equal to unity) were used. Thus, for all traits examined, closely related species tended to

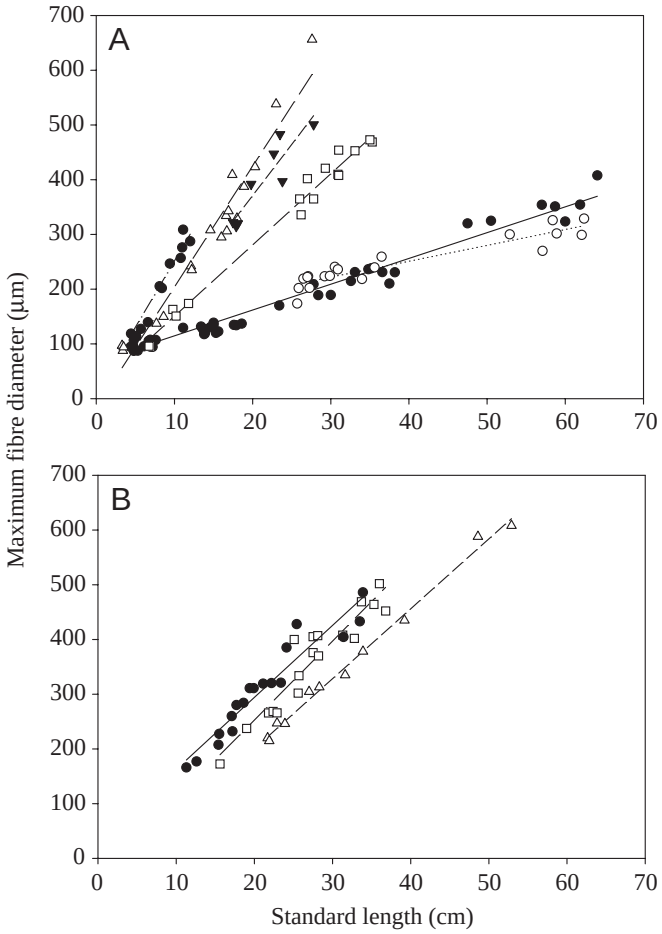

Fig. 5. The relationship between the estimated maximum fast muscle fibre diameter and standard length within nine species of Notothenioid fishes from the Southern Ocean and Patagonian shelf. (A) Antarctic Peninsula, *Notothenia coriiceps* (open squares); Shag Rocks, *Dissosticus eleginoides* (open circles); Tierra del Fuego, *Eleginops maclovinus* (filled circles), *Patagonotothen tessellata* (open triangles), *P. longipes* sp. (inverted filled triangles) and *P. sima* (filled squares). (B) Shag rocks, Icefishes *Chaenocephalus aceratus* (open triangles), *Champsocephalus gunnari* (open squares); Tierra del Fuego, *Paratonothenia magellanica* (closed circles).

Table 2. *Regression statistics for the linear regression of muscle fibre diameter on standard length, and the estimated maximum fibre diameter*

Species	d.f. residual	Intercept a	Slope b	r^2	Significance (P)	FD_{max} (μm)
Tierra del Fuego						
Eleginops maclovinus	48	67.8±3.1	4.7±0.13	0.96	<0.001	490
Paranotothenia magellanica	20	26.0±15.7	13.4±0.8	0.94	<0.001	500
Patagonotothen tessellata	16	–16.3±19.7	22.1±1.3	0.95	<0.001	600
Patagonotothen sima	6	9.2±23.8	24.3±2.5	0.94	<0.0001	300
Patagonotothen longipes sp.	6	–2.8±72.3	18.7±3.3	0.84	<0.002	550
South Georgia						
Dissosticus eleginoides	17	135.2±11.4	2.90±0.3	0.87	<0.0001	350
Chaenocephalus aceratus	9	–55.2±12.4	12.8±0.4	0.99	<0.0001	600
Champsocephalus gunnari	16	–35.7±35.6	14.4±1.3	0.89	<0.0001	500
Antarctic Peninsula						
Notothenia coriiceps	13	20.9±12.7	13.0±0.5	0.98	<0.0001	550

d.f., degrees of freedom.
FD, fibre diameter; FD_{max}, maximum fibre diameter, where FD=a+b(FD_{max}).
Values of a and b are means ± S.E.M.

have phenotypes that were more similar than for species chosen at random from the tree.

All three criteria suggested that setting all branch segments equal to unity in length was preferable for statistical analyses as compared with use of the real branch lengths. For $\log_{10}SL_{max}$, the correlation between the absolute values of the standardised contrasts and their standard deviations was –0.478 for the real branch lengths *versus* 0.190 for constant branch lengths. The corresponding MSE values were 0.162 and 0.109. Finally, r^2 in the independent contrasts regression of $\log_{10}FN_{max}$ on $\log_{10}SL_{max}$ was 0.763 *versus* 0.845. Thus, we used constant branch lengths in the following analyses.

The independent contrasts linear regression (constant branch lengths) was:

$$\log_{10}FN_{max} = 3.17 + \log_{10}SL_{max} \times 0.964$$
$$(F_{1,14}=35.0,\ P<0.0001;\ r^2=0.71)$$

With constant branch lengths, the K statistic was 0.76 for $\log_{10}SL_{max}$ and 2.81 for $\log_{10}$size-corrected FN_{max}. The former value is typical for measures of body size of a variety of organisms as compiled in Blomberg et al. (2003), but the latter is higher than any of the 35 values for morphological traits (size-corrected when necessary) that they report (range=0.29–2.22). Thus, $\log_{10}$size-corrected FN_{max} shows a relatively strong tendency for related species to resemble each other.

Finally, we tested the hypothesis that size-corrected FN_{max} was significantly lower at node 6 (supported by 88 out of 100 bootstraps) than at node 2 (supported by 100 out of 100 bootstraps), which would indicate an overall reduction in fibre number in the lineages leading to node 2. Because FN_{max} is strongly related to SL_{max} (see above and Fig. 7), we also compared SL_{max} at node 6 and node 2. The calculated 95% c.l. assuming constant branch lengths are shown in Table 3. The 95% c.l. of $\log_{10}SL_{max}$ at node 2 overlapped with that for node 6, indicating no significant difference in the estimated nodal values. However, the 95% c.l. at node 2 for size-corrected $\log_{10}FN_{max}$ do not overlap those for node 6, and so values at the two nodes can be considered significantly different. Thus, there has been a trend for the reduction of size-corrected FN_{max} but not SL_{max} in the lineages leading to node 6.

Discussion

Skeletal muscle fibres are differentiated multicellular structures specialised for contraction. It is generally accepted that the mechanism for increasing fibre number during the postembryonic stages involves the activation of myogenic precursor cells, which proliferate before leaving the cell cycle

Table 3. *Estimated ancestral values of log_{10} maximum standard length (SL_{max}) and body size-corrected maximum fibre number (FN_{max}) at nodes 2 and 6 of the phylogenetic tree estimated for notothenioid fishes*

Node	Lower 95% c.l.	Value	Upper 95% c.l.
$\log_{10}SL_{max}$			
2	1.58	1.90	2.22
6	1.27	1.58	1.89
$\log_{10}$body size-corrected FN_{max}			
2	3.01	3.20*	3.40
6	2.28	2.47	2.66

Branch lengths were set equal to unity for these analyses (see text).
c.l., confidence limit.
*Significantly different at the P<0.05 level.

and fusing to form new myotubes (Koumans and Akster, 1995; Johnston, 2001). However, some early studies failed to find candidate myogenic cells and it was proposed that in fish additional muscle fibres could also be produced by a process of splitting or budding in the mullet *Mugil cephalus* (Carpené and Veggetti, 1981) and European eel *Anguilla anguilla* (Willemse and Lieuwma-Noordanaus, 1984). This suggestion remains highly controversial, and cells with the ultrastructural characteristics of myogenic precursors were subsequently reported in the European eel (Romanello et al., 1987) and other species (Stoiber and Sänger, 1996). In the present study, we found that fast muscle fibres became subdivided in the largest specimens of three species of notothenioid studied, leading to a small increase in fibre number (Fig. 3B,C). The appearance of these subdivided fibres, which were surrounded by a network of collagen fibrils, was quite distinct from the pattern of fibre diameters observed following either stratified or mosaic hyperplasia. Subdivision was not restricted to fibres that had reached the maximum diameter and further investigation is required to determine whether 'fibre splitting' is a normal growth process or related to some pathological phenomenon such as a parasitic infection.

The notothenioid fishes comprise 8 families, 48 genera and 139 species (Balushkin, 2000) or, more conservatively, 8 families, 43 genera and 122 species (Eastman and Eakin, 2000). Cladistic analysis of osteological features has contributed to resolving notothenioid familial relationships (Iwami, 1985). There have been several phylogenies based on nucleotide sequencing of mitochondrial 12S and 16S rRNA (Bargelloni et al., 1994; Ritchie et al., 1997) and nuclear 28S rRNA (Lecointre et al., 1997). These molecular phylogenies implied extensive paraphyly, especially in the Bovichtidae and Nototheniidae. Bovichtid species were placed at the base of the tree in the sub-Antarctic zone whilst the 'core' notothenioids are largely Antarctic (Bargelloni et al., 2000). Based on mtDNA sequences, the diversification of this clade is estimated at 15–20 million years (my) ago and after the formation of the

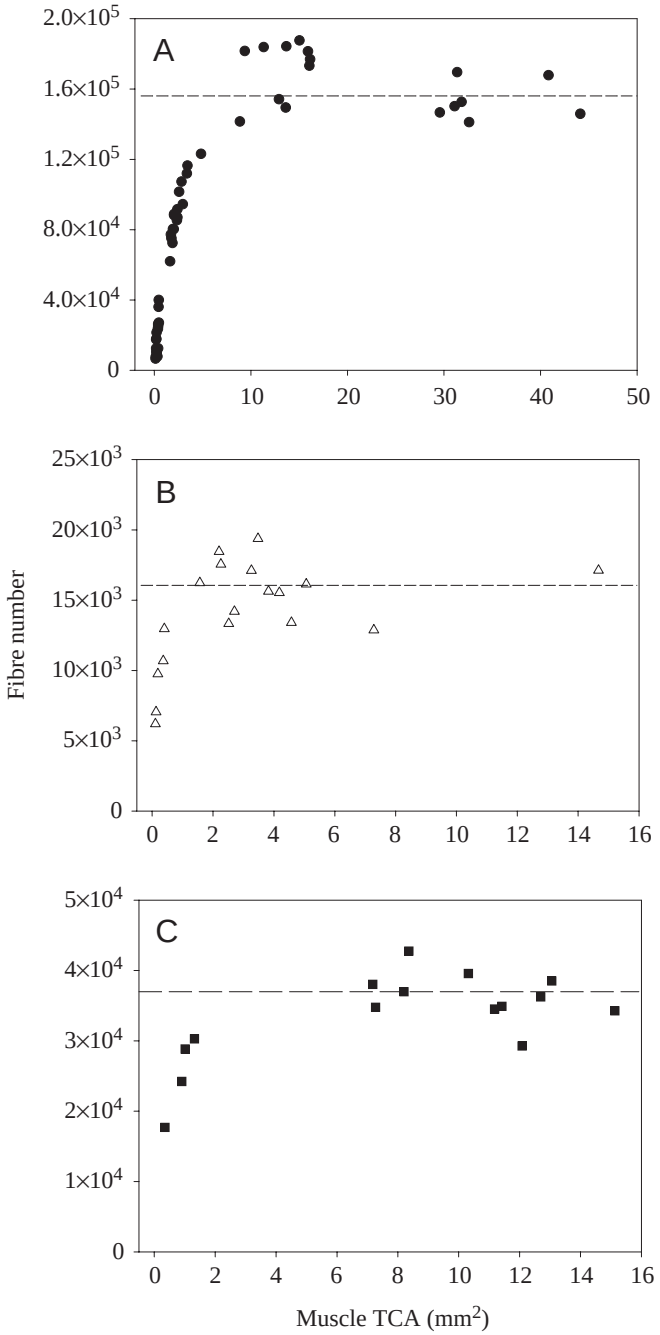

Fig. 6. (A–C). The relationship between the number of muscle fibres and the total cross-sectional area (TCA) of fast muscle at 0.7 standard length (*SL*). (A) *Eleginops maclovinus*, (B) *Patagonotothen tessellata* and (C) *Notothenia coriiceps*. The broken lines represent the estimate of FN_{max}.

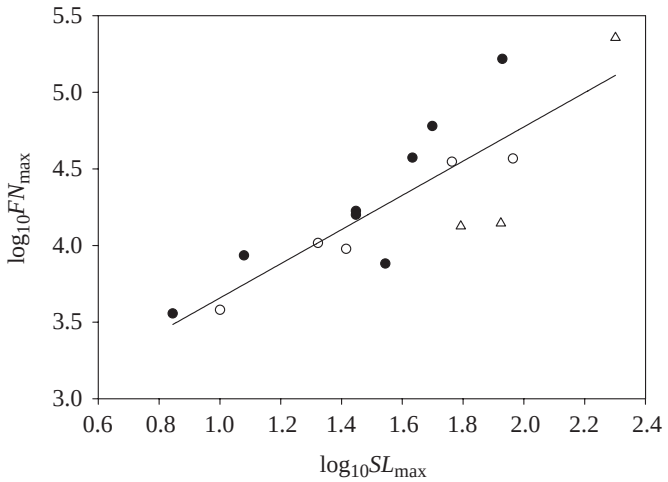

Fig. 7. The relationship between $\log_{10}$ maximum fibre number (FN_{max}; data from Fig. 8) and $\log_{10}$ maximum standard length (SL_{max}; data from Table 1) among 16 species of notothenioid fishes from Tierra del Fuego (filled circles), Shag Rocks, South Georgia (open triangles) and the Antarctic Peninsula (open circles). A conventional least-squares linear regression was fitted to the data. The equation was: $\log_{10}FN_{max}=2.53+\log_{10}SL_{max}\times1.12$ ($F_{1,14}=30.8$, $P<0.0001$; $r^2=0.69$).

Antarctic Polar Front and climatic cooling (Bargelloni et al., 2000). The phylogeny reported in Fig. 8 was in broad agreement with previous studies and assumed that *C. gobio* was the most basal of the species studied. The bootstrap support values from the Phylip analysis are shown in Fig. 8. The family Nototheniidae is probably paraphyletic, whereas Hapagiferidae and Channichthyidae are monophyletic.

The Antarctic continental shelf waters have been less than 5°C for about 12 my and today approach –1.86°C all the year around (Clarke and Crame, 1989). Notothenioids comprise 55% of fish species from the continental shelf and upper continental slope of Antarctica and often represent in excess of 90% of the species collected (Eastman, 1993; Eastman and Eakin, 2000; Clarke and Johnston, 1996; Montgomery and Clements, 2000). It has been argued that the low competitive environment under which the notothenioid radiation has occurred has allowed a higher tolerance of disaptation (evolutionary loss of function) than in other species flocks (Clarke and Johnston, 1996; Montgomery and Clements, 2000). Examples of disaptation include the loss of respiratory pigments in channichthyids and the incomplete canal formation in the lateral line associated with secondary pelagicism and paedomorphosis (Montgomery and Clements, 2000).

The present study has shown that the radiation of the group has also been associated with a progressive loss in the body size-specific maximum number of fast fibres in the myotomal muscles (FN_{max}) of the more derived species, e.g. node 6

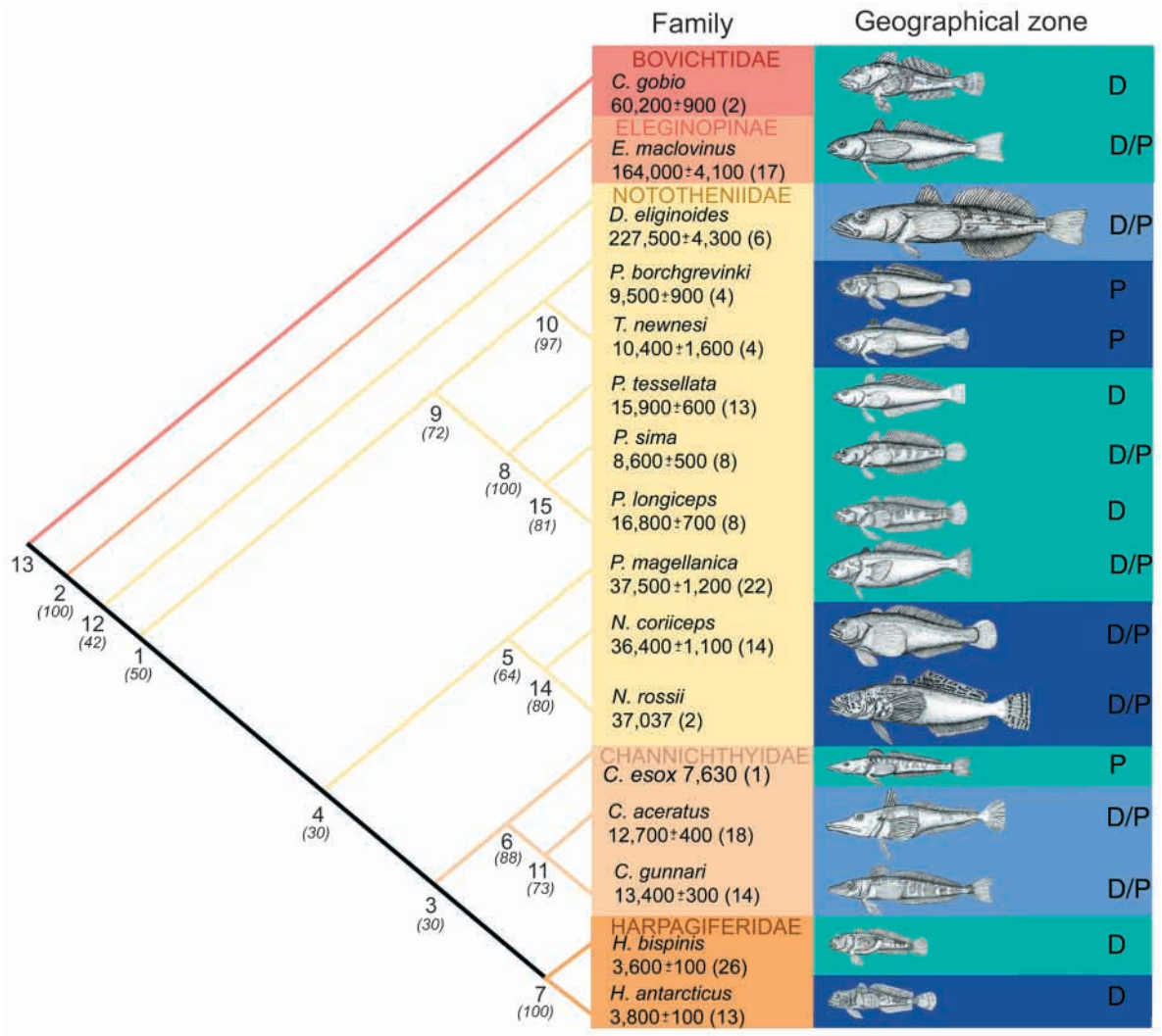

Fig. 8. Maximum likelihood phylogenetic tree estimated from 12S mitochondrial rRNA sequences and the trait values for the final number of fast muscle fibres (FN_{max}) for the notothenioid fishes studied using Phylip. Values are means ± S.E.M. (number of individuals). The bootstrap support values obtained from the Phylip analysis are shown italicised in parentheses by the nodes (see text for details). The branch lengths and node heights for the tree are given in the Appendix. The size of the fish gives some indication of their relative sizes, but they are not drawn to scale. The locomotory habit of each species is also shown: D, demersal; D/P, demerso-pelagic and P, pelagic. The colours on the right-hand side show the geographical zone of capture for each species: Beagle Channel (green), Shag Rocks, South Georgia (light blue) and Antarctic Peninsula (dark blue). The colours on the left-hand side indicate the current taxonomic families, some of which are not monophyletic.

versus node 2 in Fig. 8. The maximum standard length (SL_{max}) was a good predictor of FN_{max}, explaining about 70% of the variation observed among the 16 species studied (Fig. 7). Both $\log_{10}SL_{max}$ and the size-corrected values of $\log_{10}FN_{max}$ showed highly significant phylogenetic signal ($P<0.001$), and the amount of phylogenetic signal was unusually high for the latter trait. Thus, considering all 16 species in the study, related species tended to resemble each other with respect to both traits. However, the 95% c.l. for the estimated ancestral value of $\log_{10}SL_{max}$ at node 2, representing the ancestor at the base of the notothenioid radiation, overlapped with node 6, representing the ancestor of the Channichthyidae, one of the more derived families (Fig. 8). This suggests that there has been no general trend for a reduction in body size during the radiation of the group. Indeed, the ancestral condition is generally thought to have been a small benthic species (Eastman, 1993). In contrast, there was statistical evidence for a reduction in $\log_{10}$size-corrected FN_{max} between node 2 and node 6, consistent with a general trend for reduced fibre number in the more derived species. Thus, one of the largest species studied, *Chaenocephalus aceratus*, which reaches 85 cm SL_{max}, had only 12 700 fast muscle fibres per trunk cross-section, or 7.7% of the 164 000 fibres in *E. maclovinus*, which reaches a similar size (Fig. 8). For comparison, Atlantic salmon (*Salmo salar* L.) (Salmonidae) of 50–70 cm *SL* have 550 000–1200 000 fast muscle fibres per trunk cross-section (Johnston et al., 2000).

An important consequence of the reduction in fibre number in the more derived lineages of notothenioid fish is an increase in their maximum diameter, which can reach 600 μm in some species depending on their final body size (Fig. 5). Aerobic muscle fibre types (slow muscles) that depend on oxygen delivery to support their contractile activity also have correspondingly high maximum diameters in some Antarctic fish, and can reach 100 μm (Archer and Johnston, 1991; Smialovska and Kilarski, 1981). Whether the maximum numbers of slow and fast muscle fibres show a parallel reduction across the group remains to be determined. For Atlantic cod, fibres attain a maximum diameter of 50 μm in slow and 130 μm in fast muscle at 83 cm *SL* (Greer-Walker, 1970). FD_{max} is approx. 220 μm in Atlantic salmon and is attained at around 50 cm *SL* and (Johnston et al., 2000). The maximum muscle fibre diameter in the highly active tropical top predator, the Pacific Blue Marlin (*Makaira nigricans* Lacopóde 1803), is 50 μm for slow and 120 μm for fast muscle, even in fish exceeding 100 kg total mass (I. A. Johnston, unpublished observations). Although the comparative data are limited, the large maximum diameter of muscle fibres in notothenioid fish does appear to be exceptional.

Interestingly, the pattern of fibre diameters observed in the juvenile and adult stages of two recently diversified families of notothenioids, the Channichthyidae and the Harpagiferidae, was not consistent with the involvement of the mosaic hyperplasia phase of muscle fibre recruitment. This was confirmed using laboratory reared *H. antarcticus.* Fibre number was found to increase only twofold between the yolk-sac larvae and adult stages, and postembryonic muscle growth was entirely supported by fibre recruitment from localised germinal zones (stratified hyperplasia) (Johnston et al., 2002). Several characteristics of notothenioids, including the long pelagic larval stage of many Antarctic species, the attainment of sexual maturity at a large proportion of maximum size, the lack of haemoglobin in channichthyids, the lack of scales in channichyids and many bathydraconids (reviewed in Montgomery and Clements, 2000) and the reliance of embryonic and stratified hyperplasia during for growth in adult stages, indicate that paedomorphy has been important in notothenioid evolution.

Basic geometry dictates that an evolutionary increase in muscle fibre diameter will decrease the surface-to-volume ratio of muscle fibres. This can be expected to decrease basal energy requirements because of the concomitant reduction in membrane leak pathways, which would mean that fewer energy-utilising pumps were required to maintain ionic equilibria (Hochachka, 1986). It has been estimated that up to 40% of basal energy requirements are required to maintain ionic gradients (Jobling, 1994). Clarke and Johnston (1999) summarised literature data on the metabolic rate of different fish taxa and found a significant curvilinear relationship with temperature. However, there was no evidence that notothenioids departed from the general trend of metabolic rate with temperature in Perciformes (Johnston et al., 1991; Clarke and Johnston, 1999; Steffensen, 2002). Notothenioid fish have additional energy costs compared with other Perciformes associated with the synthesis of glycopeptide antifreezes, which are present at high concentrations in the plasma and other body fluids (Cheng and DeVries, 1991). It is possible that reductions in other aspects of basal metabolism, e.g. in relation to the loss of fibre number, serve to compensate for the additional energy costs associated with antifreeze production.

Several ‘core’ notothenioid species, including the icefish *C. esox* and species from the genus *Patagonotothen*, are found outside the Antarctic, mainly in Patagonian waters (DeWitt et al., 1976). The theory of an Antarctic origin for sub-Antarctic notothenioids is supported by the distribution of antifreeze genes among representative species (Cheng, 2000). It has been suggested that the presence of closely related species on either side of the APF represents ‘jump dispersal’ associated with episodes of climatic change rather than passive vicariance (Bargelloni et al., 2000). However, it is noteworthy that several species of notothenioids, including *C. gunnari*, which occur in the Antarctic, are also found at some islands immediately to the north of the APF (Fisher and Hureau, 1985). The relatively recent origin of the derived sub-Antarctic notothenioids (Notothenidae and Channichthyidae) would then explain why they have a relatively low muscle fibre number and high maximum diameter, traits that originated in a colder and more stenothermal environment. *E. maclovinus* and *C. gobio* have a greater size-corrected FN_{max} than the other notothenioids studied, indicating that they are

probably the least derived species. Thus *E. maclovinus* and *C. gobio* probably diverged from the other notothenioids with the separation of South America from Antarctica around 25–20 million years ago, and did not subsequently invade from Antarctica. This is probably the general case for Bovichtidae, Pseudaphritidae and Eleginopidae, since they are all represented by non-Antarctic species that lack antifreezes, except for a single Antarctic species of bovichtid (Eastman and Eakin, 2000).

The rate of oxygen delivery to aerobic muscle fibres is a function of the fibre diameter and factors that affect diffusion rate (Egginton et al., 2002). The latter include temperature, the distribution of mitochondria and lipid droplets within the fibre, and overall metabolic demand (Desaulniers et al., 1996; Londraville and Sidell, 1990; Egginton et al., 2002; O'Brien et al., 2003). The temperature-dependence of the state 3 respiration rate of isolated mitochondria with pyruvate as substrate was described by a single quadratic relationship for all Perciformes studied, with no significant upregulation of the maximum rate of oxygen uptake per mg mitochondrial protein in Antarctic and sub-Antarctic species (Johnston et al., 1998). Adequate oxygen delivery to large-diameter muscle fibres is probably only possible because of the very low metabolic demand in polar fishes at low temperature (Johnston et al., 1991; Clarke and Johnston, 1997; Steffensen, 2002). Modelling studies indicate that a low fibre number and high maximum fibre diameter does not limit adequate oxygen flux at low body temperatures (–2 to +5°C) in notothenioids (Egginton et al., 2002). There is evidence that heat death in Antarctic fish is linked to an oxygen limitation, resulting from a mis-match in oxygen delivery and consumption at the tissue level (Pörtner, 2002; Mark et al., 2002). Thus, a high FD_{max} may well constrain the upper thermal limit of notothenioids, particularly in the case of the icefish *C. esox* and other Channichthyids that lack respiratory pigments (Egginton et al., 2002).

Appendix

The phylogenetic tree was constructed using the Maximum Likelihood method with molecular clock using Phylip version 3.6a2.1. Empirical base frequencies were: A, 0.27453; C, 0.25691; G, 0.24153; T(U), 0.22702. Transition/transversion ratio=2.410000.

Discrete approximation to gamma distributed rates

Coefficient of variation of rates = 2.040000 (α=0.240292).

State in HMM	Rate of change	Probability
1	0.358	0.898
2	6.315	0.099
3	21.297	0.0024.

Ln Likelihood = –1352.86178.
HMM, hidden Markov model.

		Node	
Ancestor	Node	Height	Length
Root	13		
13	Cgob-BOV	0.25669	0.25669
13	2	0.20168	0.20168
2	Emac-NOT	0.25669	0.05501
2	12	0.20438	0.00270
12	Dele-NOT	0.25669	0.05231
12	1	0.20444	0.00006
1	9	0.22476	0.02032
9	10	0.24728	0.02252
10	Pbor-NOT	0.25669	0.00941
10	Tnew-NOT	0.25669	0.00941
9	8	0.24873	0.02397
8	Ptes-NOT	0.25669	0.00796
8	15	0.25268	0.00395
15	Psim-NOT	0.25669	0.00401
15	Plon-NOT	0.25669	0.00401
1	4	0.22386	0.01942
4	5	0.23644	0.01258
5	Pmag-NOT	0.25669	0.02025
5	14	0.24895	0.01251
14	Ncor-NOT	0.25669	0.00774
14	Nros-NOT	0.25669	0.00774
4	3	0.22938	0.00552
3	6	0.24280	0.01342
6	Ceso-CHA	0.25669	0.01389
6	11	0.24741	0.00461
11	Cace-CHA	0.25669	0.00928
11	Cgun-CHA	0.25669	0.00928
3	7	0.25544	0.02605
7	Hbis-HAR	0.25669	0.00125
7	Hant-HAR	0.25669	0.00125

This work was supported by a grant (GR3/12550) from the Natural Environment Research Council of the UK and by the Antorchas Foundation, Argentina. D.F. was in receipt of support from CONICET, Argentina, an Antorchas-British Council award for studies in the UK and from the Russell Trust Development Fund, University of St Andrews. T.G. was supported by US National Science Foundation grant DEB-0196384. We thank Dr F. E. Stockdale, Stanford University for kindly providing the S-58 and F-59 antibodies. We are grateful to Dr Inigo Everson for his help in obtaining fish from South Georgia.

References

Acierno, R., MacDonald, J. A., Agnisola, C. and Tota, B. (1995). Blood volume in the haemoglobinless Antarctic teleost *Chionodraco hamatus* (Lonnberg). *J. Exp. Zool.* **272**, 407-409.

Archer, S. D. and Johnston, I. A. (1991). Density of cristae and distribution of mitochondria in the slow muscles of Antarctic fish. *Physiol. Zool.* **64**, 242-258.

Balushkin, A. V. (2000). Morphology, classification, and evolution of notothenioid fishes of the Southern Ocean (Notothenioidei, Perciformes). *J. Ichthyol.* **40 (Suppl. 1)**, S74-S109.

Bargelloni, L., Ritchie, P. A., Patarnello, T., Battaglia, B., Lambert, D. M. and Meyer, A. (1994). Molecular evolution at subzero temperatures: mitochondrial and nuclear phylogenies of fishes from Antarctica (suborder

Notothenioidei), and the evolution of antifreeze glycopeptides. *Mol. Biol. Evol*. **11**, 854-863.

Bargelloni, L., Marcato, S., Zane, L. and Patarnello, T. (2000). Mitochondrial phylogeny of notothenioids: a molecular approach to Antarctic fish evolution and biogeography. *Syst. Biol*. **49**, 114-129.

Battram, J. C. and Johnston, I. A. (1991). Muscle growth in the Antarctic teleost, *Notothenia neglecta* (Nybelin). *Antarct. Sci*. **3**, 29-33.

Blomberg, S. P. and Garland, T., Jr (2002). Tempo and mode in evolution: phylogenetic inertia, adaptation and comparative methods. *J. Evol. Biol*. **15**, 899-910.

Blomberg, S. P., Garland, T., Jr and Ives, A. R. (2003). Testing for phylogenetic signal in comparative data: behavioural traits are more labile. *Evolution* **57**, 717-745.

Carpenè, E. and Veggetti, A. (1981). Increase in muscle fibres in the lateralis muscle (white portion) of Mugilidae (Pisces, Teleostei). *Experentia* **37**, 191-193.

Cheng, C. C. and DeVries, A. L. (1991). The role of antifreeze glycopeptides and peptides in the freezing avoidance of cold-water fish. In *Life Under Extreme Conditions: Biochemical Adaptation* (ed. G. di Prisco), pp. 1-14. Berlin and Heidelberg: Springer-Verlag.

Cheng, C. H. C. (2000). Antifreeze glycoprotein genes in temperate water notothenioid fish infer an Antarctic origin of speciation. *Am. Zool*. **40**, 972-973.

Clarke, A. and Crame, J. A. (1989). The origin of the Southern Ocean marine fauna. In *Origins and Evolution of the Antarctic Biota.* Geological Society Special Publication No. 47 (ed. J. A. Crame), pp. 253-268. London: Geological Society of London.

Clarke, A. and Johnston, I. A. (1996). Evolution and adaptive radiation of Antarctic fishes. *Trends Ecol. Evol*. **11**, 212-218.

Clarke, A. and Johnston, N. M. (1999). Scaling of metabolic rate with body mass and temperature in teleost fish. *J. Animal Ecol.* **68**, 893-905.

Cocca, E., Ratnayake-Lecamwasam, M., Parker, S. K., Camardella, L., Ciaramella, M., diPrisco, G. and Detrich, III, H. W. (1995). Genomic remnants of a-globin genes in the hemoglobinless Antarctic icefishes. *Proc. Natl. Acad. Sci. USA* **92**, 1817-1821.

Crow, M. T. and Stockdale, F. E. (1986). Myosin expression and specialization among the earliest muscle fibres of the developing avian limb. *Dev. Biol*. **113**, 238-254.

Desaulniers, N., Moerland, T. S. and Sidell, B. D. (1996). High lipid content enhances the rate of oxygen diffusion through fish skeletal muscle. *Am. J. Physiol*. **271**, R42-R47.

Devoto, S. H., Melacon, E., Eisen, J. S. and Westerfield, M. (1996). Identification of separate slow and fast muscle precursor cells *in vivo*, prior to somite formation. *Development* **122**, 3371-3380.

DeWitt, H., McCleave, J. D. and Dearborn, J. H. (1976). Ecological studies of fishes and echinoderms during ARA Islas Orcadus cruise 5. *Antarct. J. US* **11**, 49-53.

Díaz-Uriarte, R. and Garland, T., Jr (1998). Effects of branch length errors on the performance of phylogenetically independent contrasts. *Syst. Biol*. **47**, 654-672.

Dunn, J. S. D., Archer, S. D. and Johnston, I. A. (1989). Muscle fibre types and metabolism in postlarval and adult stages of Notothenioid fish. *Polar Biol*. **9**, 213-223.

Eastman, J. T. (1993). *Antarctic Fish Biology: Evolution in a Unique Environment.* 322p. San Diego: Academic Press.

Eastman, J. T. (1997). Phyletic divergence and specialization for pelagic life in the Antarctic notothenioid fish *Pleuragramma antarcticum*. *Comp. Biochem. Physiol*. **118A**, 1095-1101.

Eastman, J. T. and Eakin, R. R. (2000). An updated species list for notothenioid fish (Perciformes; Notothenioidei), with comments on Antarctic species. *Arch. Fish. Mar. Res.* **48**, 11-20.

Egginton, S., Stilbeck, C., Hoofd, L., Calvo, J. and Johnston, I. A. (2002). Peripheral oxygen transport in skeletal muscle of Antarctic and sub-Antarctic notothenioid fish. *J. Exp. Biol.* **205**, 769-779.

Felsenstein, J. (1985). Phylogenies and the comparative method. *Am. Nat.* **125**, 1-15.

Fernández, D. A., Calvo, J., Franklin, C. E. and Johnston, I. A. (2000). Muscle fibre types and size distribution in sub-Antarctic notothenioid fishes. *J. Fish Biol*. **56**, 1295-1311.

Fisher, W. and Hureau, J. C. (1985). *FAO Species Identification Sheets for Fishery Purposes, Southern Ocean*, vol 2. Rome, Italy: FAO.

Freckleton, R. P., Harvey, P. H. and Pagel, M. (2002). Phylogenetic analysis and comparative data: a test and review of evidence. *Am. Nat*. **160**, 712-726.

Garland, T., Jr, Harvey, P. H. and Ives, A. R. (1992). Procedures for the analysis of comparative data using phylogentically independent contrasts. *Syst. Biol*. **4**1, 18-32.

Garland, T., Jr, Midford, P. E. and Ives, A. R. (1999). An introduction to phylogenetically based statistical methods, with a new method for confidence values on ancestral values. *Am. Zool*. **39**, 374-388.

Gon, O. and Heemstra, P. C. (ed.) (1990). In *Fishes of the Southern Ocean.* Grahamstown, South Africa: J. L. B. Smith Institute of Ichthyology.

Greer-Walker, M. G. (1970). Growth and development of the skeletal muscle fibres of the cod (*Gadus morhua* L.). *J. Cons. Perm. Int. Explor. Mer.* **33**, 228-244.

Hall, T. A. (1999). BioEdit: a user-friendly biological sequence alignment editor and analysis program for Windows 95/98/NT. *Nucl. Acids. Symp. Ser.* **41**, 95-98.

Hochachka, P. W. (1986). Defense strategies against hypoxia and hypothermia. *Science* **231**, 234-241.

Iwami, T. (1985). Osteology and relationships of the family Channichthyidae. *Mem. Natl. Inst. Polar Res. Ser. E*, pp. 1-69.

Jobling, M. (1994). *Fish Bioenergetics.* London: Chapman and Hall.

Johnston, I. A. (1987). Respiratory characteristics of muscle fibres in a fish (*Chaenocephalus aceratus*) that lacks respiratory pigments. *J. Exp. Biol.* **133**, 415-428.

Johnston, I. A. (1989). Antarctic fish muscles-structure, function and physiology. *Antarct. Sci.* **1**, 97-108.

Johnston, I. A. (2001). Genetic and environmental determinants of muscle growth patterns. In *Muscle Development and Growth*. *Fish Physiology*, vol. 18 (ed. I. A. Johnston), pp. 141-186. San Diego: Academic Press.

Johnston, I. A., Calvo, J., Guderley, H., Fernández, D. A. and Palmer, L. (1998). Latitudinal variation in the abundance and oxidative capacities of muscle mitochondria in Perciform fishes. *J. Exp. Biol.* **210**, 1-12.

Johnston, I. A., Clarke, A. and Ward, P. (1991). Temperature and metabolic rate in sedentary fish from the Antarctic, North Sea and Indo-West Pacific Ocean. *Mar. Biol*. **109**, 191-195.

Johnston, I. A., Fitch, N., Zummo, G., Wood, R. E., Harrison, P. and Tota, B. (1993). Morphometric and ultrastructural features of the ventricular myocardium of the haemoglobin-less icefish, *Chaenocephalus aceratus*. *Comp. Biochem. Physiol*. **76A**, 475-480.

Johnston, I. A., Manthri, S., Robertson, B., Campbell, P., Mitchell, D. and Alderson, R. (2000). Family and population differences in muscle fibre recruitment in farmed Atlantic salmon (*Salmo salar*). *Basic Appl. Myol*. **10**, 291-296.

Johnston, I. A., Strugnell, G., McCraken, M. L. and Johnstone, R. (1999). Muscle growth and development in normal-sex-ratio and all-female diploid and triploid Atlantic salmon. *J. Exp. Biol.* **202**, 1991-2016.

Johnston, I. A., Vieira, V. L. A., Fernández, D. A., Abercromby, M., Brodeur, J. C., Peck, L. and Calvo, J. (2002). Muscle growth in polar fish: a study of Harpagifer species with sub-Antarctic and Antarctic distributions. *Fish. Sci*. **68 Suppl. II**, 1023-1028.

Klingenberg, C. P. and Ekau, W. (1996). A combined morphometric and phylogenetic analysis of an ecomorphological trend: pelagization in Antarctic fishes (Perciformes; Notothenioidei). *Biol. J. Linn. Soc*. **59**, 143-177.

Koumans, J. T. M. and Akster, H. A. (1995). Myogenic cells in development and growth of fish. *Comp. Biochem. Physiol*. **110A**, 3-20.

Lecointre, G., Bonillo, C., Ozouf-Costaz, C. and Hureau, J. C. (1997). Molecular evidence for the origins of Antarctic fishes: paraphyly of the Bovichtidae and no indication of monophyly of the Notothenioidei (Teleostei). *Polar Biol*. **18**, 193-208.

Londraville, R. L. and Sidell, B. D. (1990). Ultrastructure of aerobic muscle in Antarctic fishes may contribute to diffusive fluxes. *J. Exp. Biol.* **150**, 205-220.

Mark, F. C., Bock, C. and Pörtner, H. O. (2002). Oxygen-limited thermal tolerance in Antarctic fish investigated by MRI and ^{31}P-MRS. *Am. J. Physiol. Regul. Integr. Comp. Physiol.* **283**, R1254-R1262.

Montgomery, J. and Clements, K. (2000). Disaptation and recovery in the evolution of Antarctic fishes. *Trends Ecol. Evol*. **15**, 267-271.

Moylan, T. J. and Sidell, B. D. (2000). Concentrations of myoglobin and myoglobin mRNA in heart ventricles from Antarctic fishes. *J. Exp. Biol.* **203**, 1277-1286.

O'Brien, K. M. O., Skilbeck, C., Sidell, B. D. and Egginton, S. (2003). Muscle fine structure may maintain the function of oxidative fibres in haemoglobinless Antarctic fishes. *J. Exp. Biol.* **206**, 411-421.

Pörtner, H. O. (2002). Physiological basis of temperature-dependent

biogeography: trade-offs in muscle design and performance in polar ectotherms. *J. Exp. Biol.* **205**, 2217-2230.

Reynolds, R. W. and Smith, T. M. (1994). Improved global sea surface temperature analyses. *J. Climate* **7**, 929-948

Ritchie, P. A., Lavoue, S. and Lecointre, G. (1997). Molecular phylogenetics and the evolution of Antarctic notothenioid fishes. *Comp. Biochem. Physiol.* **118**, 1009-1025.

Romanello, M. G., Scapolo, P. A., Luprano, S. and Mascarello, F. (1987). Post-larval growth in the lateral white muscle of the eel, *Anguilla anguilla*. *J. Fish Biol.* **30**, 161-172.

Rowlerson, A., Mascarello, F., Radaelli, G. and Veggetti, A. (1995). Differentiation and growth of muscle in the fish *Sparus aurata* (L.): II Hyperplastic and hypertrophic growth of lateral muscle from hatching to adult. *J. Mus. Res. Cell Motil.* **16**, 223-236.

Rowlerson, A. and Veggetti, A. (2001). Cellular mechanisms of post-embryonic muscle growth in aquaculture species. In *Muscle Development and Growth. Fish Physiology*, vol. 18 (ed. I. A. Johnston), pp. 103-140. San Diego: Academic Press.

Small, D. J., Moylan, T., Vayda, M. E. and Sidell, B. D. (2003). The myoglobin gene of the Antarctic icefish, *Chaenocephalus aceratus*, contains a duplicated TATAAAA sequence that interferes with transcription. *J. Exp. Biol.* **206**, 131-139.

Smialowska, E. and Kilarski, W. (1981). Histological analysis of fibers in myotomes of Antarctic fish (Admiralty Bay, King George Island, South Shetland Islands). I. Comparative analysis of muscle fiber size. *Pol. Polar Res.* **2**, 109-129.

Stankovic, A., Spalik, K., Kamler, E., Borsuk, P. and Weglenski, P. (2001). Recent origin of sub-Antarctic notothenioids. *Polar Biol.* **25**, 203-205.

Steffensen, J. F. (2002). Metabolic cold adaptation of polar fish based on measurements of aerobic oxygen consumption: fact or artefact? Artefact! *Comp. Biochem. Physiol.* **132A**, 789-795.

Stoiber, W. and Sänger, A. M. (1996). An electron microscopic investigation into the possible source of new muscle fibres in teleost fish. *Anat. Embryol.* **194**, 569-579.

Tota, B., Cerra, M. C., Mazza, R., Pellegrino, D. and Icardo, J. (1997). The heart of the antarctic icefish as paradigm of cold adaptation. *J. Therm. Biol.* **22**, 409-417.

Vayda, M. E., Small, D. J., Yuan, M., Costello, L. and Sidell, B. D. (1997). Conservation of the myoglobin gene among Antarctic notothenioid fishes. *Mol. Mar. Biol. Biotechnol.* **6**, 207-216.

Weatherley, A. H., Gill, H. S. and Lobo, A. F. (1988). Recruitment and maximum diameter of axial muscle fibres in teleosts and their relationship to somatic growth and ultimate size. *J. Fish Biol.* **33**, 851-859.

Willemse, J. J. and Lieuwma-Noordanus, C. (1984). The generation of 'new' white muscle fibres by budding in the lateral musculature of elvers, *Anguilla anguilla* (L.) during normal development. *Experientia* **40**, 990-992.